Journal of Molecular Spectroscopy 415 (2026) 112068

Contents lists available at ScienceDirect

Journal of Molecular Spectroscopy

journal homepage: www.elsevier.com/locate/yjmsp

High-accuracy solution of the rovibrational Schrödinger equation for triatomic molecules

Roman I. Ovsyannikov [a], Armando N. Perri [b], Irina I. Mizus [a], Jonathan Tennyson [b], Sergei N. Yurchenko [b], Alexander O. Mitrushchenkov [c], Nikolai F. Zobov [a], Mikhail A. Rogov [a,d], Oleg L. Polyansky [b,a,*]

[a] Institute of Applied Physics, Russian Academy of Sciences, 46 Ulyanov Street, Nizhny Novgorod, 603950, Russia
[b] Department of Physics and Astronomy, University College London, Gower Street, London WC1E 6BT, United Kingdom
[c] MSME, Université Gustave Eiffel, CNRS UMR 8208, Univ Paris Est Creteil, F-77474 Marne-la-Vallée, France
[d] Department of Radiophysics, N. I. Lobachevsky State University of Nizhny Novgorod, 23 Gagarin Avenue, Nizhny Novgorod 603022, Russia

ARTICLE INFO

Keywords:
Schrödinger equation
Numerical methods
Energy levels
Einstein A coefficients
CO_2

ABSTRACT

Modern meteorological studies and atmospheric monitoring are placing stringent requirements on the accuracy of high-resolution molecular spectroscopy at infrared and visible wavelengths. Experimental progress towards accurately determining infrared line centers to within kilohertz and line intensities to better than sub-promille accuracy requires corresponding progress in theoretical determinations. Recently, it has been demonstrated that modern rovibrational programs for diatomic molecules (DUO and LEVEL) can solve the Schrödinger equation with an accuracy of 1 part in 10^8 by analysis of numerical solutions of exactly solvable problems. The demand for such agreement in triatomic calculations is pressing. Nine to ten digit convergence for computed CO_2 rovibrational energy levels is demonstrated herein using a variety of available variational nuclear motion programs based on the use of exact (within the Born–Oppenheimer approximation) kinetic energy operators. The programs DVR3D, in both Radau and Jacobi coordinates, EVEREST, RV3 and TROVE are compared. The agreement achieved corresponds to about 0.00005 cm^{-1} which sets a new benchmark for accuracy. A comparison of DVR3D and EVEREST also shows agreement for computed Einstein A coefficients at the sub-percent level for the majority of transitions.

1. Introduction

The last decade has witnessed a new era in the high-accuracy measurement of molecular absorption line positions and intensities. The typical accuracy to which line positions can be determined at infrared and visible wavelengths has improved by 2 to 3 orders of magnitude from about 0.002 cm^{-1} to better than 0.000003 cm^{-1} [1–3]. This level of accuracy has been achieved for several different molecules, not just for CO_2 considered in this work.

Recently, several infrared line positions of water [4] were measured with an accuracy of 5×10^{-5} cm^{-1}, while the lines of CO have been measured with an accuracy of about 3×10^{-7} cm^{-1} [5]. Historically, the situation has been rather different for line intensities, as the level of accuracy achieved by both experiment and theory was much lower, typically in the range 1%–20%. However, recent line intensity measurements have reduced uncertainties by one to two orders of magnitude to better than 0.1% [6–8]. Thus, line intensities accurate to better than 0.01% have been achieved for both CO_2 [8] and CO [6,9], which has been analyzed in a recent ultra-high precision study of line intensity ratios [10].

Theoretical calculations of line positions and line intensities play a significant role in the mutual support of experimental measurements. The accuracy with which rovibrational energy levels of triatomic molecules can be computed using variational nuclear motion programs depends on three main factors: First, the accuracy of solution of the eigenvalue problem for an arbitrary potential energy surface (PES); second, the accuracy of the PES itself; and third, assuming the codes use exact (nuclear motion) kinetic energy (EKE) operators, any correction to this arising from the Born–Oppenheimer approximation. The third factor makes a relatively minor contribution for molecules that do not contain hydrogen atoms; recent MARVEL (Measured Active Rotation–Vibration Energy Level) studies of symmetric and asymmetric isotopologues of CO_2 suggest that neglect of non-adiabatic effects in the Ames-2 PES used here gives rise to shifts in the region of 0.02 cm^{-1} [11,12]. In principle, once the first and third factors are

* Corresponding author at: Department of Physics and Astronomy, University College London, Gower Street, London WC1E 6BT, United Kingdom.
E-mail address: o.polyansky@ucl.ac.uk (O.L. Polyansky).

https://doi.org/10.1016/j.jms.2025.112068
Received 11 September 2025; Received in revised form 30 November 2025; Accepted 19 December 2025
Available online 22 December 2025

addressed, the accuracy of the PES should be limited only by the accuracy of experiment, since modern accurate PESs are fit such that their use in nuclear motion calculations reproduce empirical energy level [13].

Clearly, for high-accuracy studies, the methods used to solve the nuclear motion and associated programs become important. For example, when used in an empirical refinement of PES, any error introduced by the nuclear motion solver will, for example, become an artifact in any fitted PES hindering the approach to experimental accuracy for computed energy levels and, in particular, any predictions of unobserved line positions. This has consequences for the construction of theoretical line lists and their subsequent ability to aid in experimental line assignment. The calculation of transition intensities to high accuracy in such line lists, often included as Einstein A coefficients, introduces a fourth factor: the accuracy of the electronic dipole moment surface (DMS).

For diatomic molecules, the ability of existing nuclear motion programs Duo [14] and LEVEL [15] to solve the Schrödinger equation with high accuracy was demonstrated [16] by comparison of exactly solvable model systems. It was shown that numerical solutions for calculated line intensities were accurate to better than 10^{-6}%. It was also shown that DUO, a variational nuclear motion program that uses basis set expansions like the programs tested here, gave considerably faster convergence than LEVEL, which uses direct numerical solution of the nuclear motion Schrödinger equation. This study was also an important step towards providing highly accurate dipoles [17].

For triatomic molecules, we consider here nuclear motion programs which calculate rovibrational energy levels numerically for a given potential energy surface. These surfaces can be obtained from *ab initio* electronic structure calculations, empirically-determined by fitting to experimental data, or, as is common, a hybrid between the two approaches. There are a number of nuclear motion programs in current use that are based on the use of exact (within the Born–Oppenheimer approximation) kinetic energy operators, arbitrary potential energy surfaces and the variational principle to converge results; these include DVR3D [18], TRIATOM [19], TROVE [20,21], EVEREST [22], VTET [23], ScalIT [24], DEWE [25], RV3 [26,27] and TNUM [28]. There have been some comparisons between variational nuclear motion programs for triatomic molecules [29–32], however, although these studies gave satisfactory results, the emphasis was not on high accuracy. Given, for example, the fact that four of the top five molecules in the widely-used HITRAN database are triatomics [33], the case for developing high-accuracy procedures for triatomics is pressing.

The important molecule CO_2 is used in this work as a benchmark system. Besides its obvious importance, CO_2 has a number of advantages for both theoretical and experimental studies: it is a closed-shell triatomic with no hyperfine spectra in its main isotopologue ($^{16}O^{12}C^{16}O$) which is considered here. The rovibrational spectrum of CO_2 has been exceptionally well-studied [34] and has been the subject of the most accurate available measurements of its line intensities for any triatomic molecule [8].

The construction of an exactly solvable model for a triatomic that mimics the anharmonic behavior of a real system, however, is not straightforward. Our procedure for validating the accuracy of triatomic calculations is twofold. First, we demonstrate convergence with increasing size of the final Hamiltonian matrix for two different coordinate systems, Jacobi and Radau, using the program DVR3D [18]. We then demonstrate that both solutions for the energy levels converge to the same value within 10^{-6} – 10^{-5} cm^{-1}. This accuracy corresponds to 30 – 100 kHz for energy levels up to 7 000 cm^{-1}, and to 100 – 300 kHz for levels above 7 000 cm^{-1}. Secondly, we compare these results with energy levels from the rovibronic triatomic nuclear motion program EVEREST [22], the triatomic nuclear motion program RV3 [26,27] and the general nuclear motion program TROVE [20] using exactly the same PES. In this paper we report new calculations performed with DRV3D, using both Radau and Jacobi coordinates, EVEREST and TROVE; our results can be compared with similar calculations reported in literature by Wang and Carrington [27] and Huang et al. [35].

The following analysis demonstrates astonishingly good (up to 10^{-6} cm^{-1}) agreement for CO_2 rovibrational energy levels between the aforementioned programs with use of different coordinate systems. For DVR3D and EVEREST, Einstein A coefficients are also computed with sub-percent agreement for the majority of transitions considered.

Table 1
The fundamental constants, atomic masses and conversion factors used in this study.

a_0	0.529177249 Å	[27]
m_C	11.99670909 Da[a]	[27]
m_O	15.99052593 Da[a]	[27]
1 Hartree	219474.631482453 cm^{-1}	[27]
1 Da	1822.88848627814 m_e	[36]

[a] Converted from m_e to Daltons with [36].

2. General considerations

The use of variational methods for performing rotation–vibration nuclear motion calculations is well-established and has been the subject of a number of review articles [37–43]. Having formulated the problem the methodology involves selecting suitable basis functions which are integrated over to give the required Hamiltonian matrix elements. Diagonalization of the Hamiltonian matrix gives the energies and wavefunctions required. These wavefunctions can then be used to compute transition Einstein-A coefficients using appropriate dipole moment surface(s). In the discrete variable representation (DVR) approach the basis sets and integration grids are linked [38,39] meaning the approach is not strictly variational. However, with care and large enough basis sets (integration grids) the calculations behave variationally. All three codes tested here use version of the DVR method as discussed in the given citation. TROVE [20] uses internal contraction schemes to automatically generate basis functions, while DVR3D [18] uses specified basis sets which usually need to be optimized for a given molecule and coordinate scheme. DVR3D has been extensively used for high accuracy calculations on CO_2, and the basis set parameters employed here were carefully optimized previously [44]. EVEREST [22] uses a mixture of contracted (radial) basis sets and a DVR in (associated) Legendre polynomials for the bending coordinate; again, no basis set parameters other than grid and final basis set sizes are required. The rovibrational calculations of this work were performed using DVR3D with both Jacobi and Radau coordinates, as well as EVEREST with Radau coordinates, and TROVE with bond length bond angle (BLBA) coordinates.

For an accurate comparison of these programs, it was necessary to define one potential energy surface (PES) and one dipole moment surface (DMS), along with a common set of fundamental constants, atomic masses and conversion factors. All results presented below were calculated using the Ames-2 PES of Huang et al. [35] and the DMS given by Fleisher et al. [45]; FORTRAN implementations of these are provided in the supporting materials. Table 1 specifies the fundamental constants, atomic masses and conversion factors used in each calculation reported here. These constants are very close to but probably not identical to those used in the studies of Wang and Carrington [27] and Huang et al. [35].

All energy level assignments are given in AFGL (Air Force Geophysics Laboratory) notation [46,47] as used in the empirical rovibrational (MARVEL) analysis of $^{12}C^{16}O_2$ [34]. The designation (J v_1 v_2 l_2 v_3 r p) uniquely assigns each energy level, where J denotes the total angular momentum, v_1 denotes the symmetric stretch vibrational quantum number, v_2 denotes the bending vibrational quantum number, v_3 denotes the asymmetric stretch quantum number and r is an index over states in Fermi resonance counted by descending energy; in AFGL notation l_2 is fixed to v_2. Finally, p denotes the rotationless (e/f) parity: an energy level has e rotationless parity when $J + l_2 + v_3$ is even, and f rotationless parity when $J + l_2 + v_3$ is odd.

Table 2
The converged $J = 0$ even energy levels calculated using DVR3D with Jacobi and Radau coordinates in units of cm^{-1}.

Coordinates	Jacobi	Radau
2D Matrix Dimension	108 000	24 000
3D Matrix Dimension	16 000	2 000
Number of points in (r_1, θ, r_2)	60 60 60	20 120 20
r_1 Basis Parameters	4.5 0.2 0.01	2.95 0.3 0.0085
r_2 Basis Parameters	0.0 0.0 0.25	2.95 0.3 0.0085
	1285.41432850	1285.41432768
	1388.18658678	1388.18658592
	2548.36613391	2548.36613266
	2671.13964513	2671.13964460
	2797.13299362	2797.13299210
	3792.67893916	3792.67893751
	3942.52148486	3942.52148367
	4064.26212448	4064.26212307
	4225.09233870	4225.09233659
	4673.29921552	4673.29921545
	5022.36009273	5022.36009054
	5197.23344145	5197.23343954
	5329.62483658	5329.62483527
	5475.53984186	5475.53983945
	5667.63955819	5667.63955533
	5915.20501389	5915.20501263
	6016.70367861	6016.70367753
	6240.09503412	6240.09503152
	6435.51460897	6435.51460693
	6588.31810120	6588.31809980
	6725.26073039	6725.26072860
	6903.91187966	6903.91187711
	7121.72122836	7121.72122487
	7133.80560824	7133.80560600
	7259.77335403	7259.77335175
	7377.71457747	7377.71457534
	7447.70485430	7447.70485149
	7659.97759536	7659.97759316
	7834.84619686	7834.84619466
	7974.42513706	7974.42513506

3. Energy level calculations for DVR3D

DVR3D [18] solves the nuclear motion Schrödinger equation for an isolated triatomic molecule within the Born–Oppenheimer approximation using a variational approach. It utilizes a discrete variable representation (DVR) for all three coordinates (r_1, r_2, θ) [48] and uses an exact analytically-obtained kinetic energy operator [49,50]. DVR3D computes energy levels, wavefunctions and dipole transition moments for both rotational and vibrational excitations. It requires a user-defined PES for energy level calculations and a DMS for intensity calculations.

For an efficient treatment of rovibrational motion in a DVR, it is beneficial to use an orthogonal coordinate system which does not possess any off-diagonal terms in the kinetic energy operator [51]. DVR3D allows for such an orthogonal calculation using either Jacobi (scattering) or Radau coordinates, which both preserve the symmetry of an AB_2 triatomic molecule. In Jacobi coordinates, r_1 represents the diatom distance between atoms 2 and 3, and r_2 the separation of the atom 1 from the diatom center-of-mass, where the atom order for CO_2 here is C, O and O. The angle between r_1 and r_2 is θ. In Radau coordinates, r_1 and r_2 are close to valence bond length bond angle (BLBA) coordinates when the central atom is much heavier than the other two atoms. This is not the case for CO_2, but Radau coordinates have previously been found to work well for this molecule [44]. The Radau coordinate calculations used a bisector embedding while the Jacobi calculations use the r_1 embedding in DVR3D, which places the z axis along a vector connecting the two oxygen atoms. In either case, DVR3D utilizes associated Legendre polynomials as DVR basis functions for the angular degree of freedom, and either Morse-like or spherical oscillator DVR basis functions for the radial degree of freedom.

Radial basis functions used in the DVR3D algorithm have a few parameters, which have to be specified to solve a nuclear motion problem, and need to be chosen to ensure the necessary level of convergence. In principle, these parameters have a clear physical meaning, in practice they are simply used as adjustable variational parameters. For the Morse-like oscillator functions used in Radau coordinates to represent the radial motions, see Eqs. (2) and (3) of Ref. [18], the parameters r_e, ω_e and D_e can be associated with the equilibrium distance for a pair of nuclei positioned along the relevant radial coordinate, their fundamental frequency and dissociation energy [49], respectively. While for spherical oscillators, see Eqs. (4) and (5) of Ref. [18], these are the α and ω parameters of the spherical oscillator [52]; their physical interpretation is discussed further below. The various basis set and other parameters used in the DVR3D calculations are specified in Table 2 below.

Consequently, DVR3D has the programmed capability to calculate triatomic energy levels in both Radau and Jacobi coordinates. This was the starting point for our current investigation, where we aim to achieve a new level of convergence and accuracy in the solution of the rovibrational Schrödinger equation. This analysis is supported by our well-optimized parameters that are capable of achieving good convergence; those used to calculate a room temperature line list in Radau coordinates with Morse-like oscillators [44], and those used to calculate energy levels for $^{14}N_2\,^{16}O$ with a standard deviation of approximately 3×10^{-3} cm^{-1} in Jacobi coordinates using spherical oscillators [53]. We find below that the application of these respective coordinates and basis functions both converge energy levels for CO_2 to unexpectedly similar values. This agreement supports the high-accuracy claim that our calculated energy levels show convergence on the order of 10 kHz.

3.1. $J = 0$ calculations

Table 2 presents converged $J = 0$ even energy levels calculated with both Radau and Jacobi coordinates. This table shows that the two independent calculations, using different coordinate systems, basis types, basis sizes and final (3D) matrix size, converge to 6 – 8 decimal places in cm^{-1}, or 1 – 100 kHz. DVR3D can also perform an intermediate (2D) diagonalization and truncation step; in practice the full matrix, with sizes as stated, was retained in all cases.

We see also that the calculations in both coordinate systems converge monotonically to these values as a function of the final matrix size. One can see that the results coincide at the 3×10^{-6} cm^{-1} level and that further increases in size of the final matrix do not improve this agreement.

Table 3 gives the converged $J = 0$ even and odd energy levels using our final matrix sizes for both Radau and Jacobi coordinate systems. The coincidence of the results presented does not provide absolute proof of convergence of the Schrödinger equation to an exact result; nevertheless, fortuitous agreement of the two numerical solutions to the same value is extremely unlikely, and our comparison demonstrates that the accuracy of the solution of the Schrödinger equation is almost as reliable as that of previous studies on diatomic systems [16].

The fact that convergence in Radau coordinates is achieved with a smaller number of integration points and with a smaller size of the Hamiltonian matrix than in Jacobi coordinates, indicates the greater efficiency of the Radau coordinate system for this particular problem. This finding is in line with our experience; while Morse-like oscillators provide efficient basis functions that converge very quickly, spherical oscillators are inefficient and lead to large basis set requirements.

3.2. Issues with $J = 0$ odd calculations

The need to calculate $J = 0$ energy levels with odd symmetry, which do not exist in nature, arose firstly as a fundamental test of the DVR3D program; comparisons of these levels is useful for studies of other molecules, including the asymmetric isotopologues of CO_2, for which both symmetries exist. Secondly, an odd vibrational basis

Table 3
The difference between converged DVR3D $J = 0$ even energy levels in Jacobi and Radau coordinates (see Table 2) and energy levels calculated with smaller matrix dimensions in units of 10^{-8} cm^{-1}. The primitive basis set size is 108 000 for Jacobi and 24 000 for Radau.

Coordinates	Jacobi	Jacobi	Jacobi	Jacobi	Jacobi	Jacobi	Radau	Radau	Radau	Radau	Radau	Radau	Radau	Radau
3D Matrix Dimension	3000	7000	9000	10 000	13 000	16 000	2000	1500	1000	500	400	300	200	100
	127	85	85	84	86	82	0	0	0	0	0	0	3	6815
	100	90	90	88	90	86	0	0	0	0	0	1	3	3750
	990	130	130	128	130	125	0	0	0	0	0	2	119	160 157
	269	58	59	56	58	53	0	0	0	0	0	1	114	121 132
	255	158	158	156	158	152	0	0	0	0	0	1	151	176 305
	7764	171	170	169	170	165	0	0	0	1	1	24	3532	1 137 911
	2153	124	124	122	123	119	0	0	0	0	0	17	4111	1 596 620
	1266	146	146	144	146	141	0	0	0	0	0	23	5550	2 791 302
	746	216	216	214	216	211	0	0	0	0	0	39	7342	6 233 339
	529	12	13	11	12	7	0	0	0	0	1	9	3919	2 172 497
	39 868	226	223	221	223	219	0	0	0	1	9	385	60 377	14 153 606
	16 838	197	196	195	196	191	0	0	0	0	5	445	89 531	19 901 617
	7405	136	136	134	136	131	0	0	0	1	5	533	111 162	38 502 267
	6097	246	246	244	246	241	0	0	0	0	6	1026	201 033	79 279 816
	2933	291	291	289	291	286	0	0	0	0	7	2189	245 456	173 634 106
	25 016	133	132	130	131	126	0	0	0	2	26	410	242 033	36 946 513
	6767	115	114	112	113	108	0	0	0	1	9	343	147 926	96 813 150
	147 273	282	265	263	265	260	0	0	0	9	75	7040	609 536	128 162 350
	104 754	218	210	208	210	204	0	0	0	7	83	8951	1 169 867	342 423 843
	42 077	149	146	144	146	140	0	0	0	5	99	10 074	1 514 238	337 168 213
	33 951	187	185	182	184	179	0	0	0	6	155	17 210	2 791 289	864 837 708
	24 213	261	260	258	260	255	0	0	0	9	248	35 059	5 163 075	1392 395 524
	12 926	355	354	352	354	349	0	0	0	13	329	89 261	6 461 749	2190 689 682
	342 236	250	232	229	230	224	0	0	0	33	356	16 448	2 848 948	1244 663 129
	84 826	243	239	236	235	228	0	0	0	12	156	13 847	2 363 654	1375 127 110
	43 875	222	221	218	219	213	0	0	0	9	182	14 562	3 518 888	3027 811 385
	440 956	352	289	285	286	281	0	0	0	66	649	91 994	6 666 449	1801 247 650
	462 052	275	225	223	225	220	0	0	0	80	1310	128 380	10 904 170	3157 026 293
	230 642	245	235	233	235	220	0	0	0	90	2140	149 980	16 879 070	4210 116 123
	137 432	215	205	203	205	200	0	0	0	110	3120	203 490	23 829 210	5060 081 513

Table 4
The difference between DVR3D $J = 0$ odd energy levels in Jacobi coordinates and the converged Radau energy levels in units of 10^{-8} cm^{-1}; npt2 gives the number of angular DVR points and zquad2 specifies whether quadrature approximation is used (true) or not (false) for this coordinate.

Coordinates	Radau	Jacobi	Jacobi	Jacobi	Jacobi	Jacobi	Jacobi
2D Matrix Dimension	24 000	108 000	108 000	144 000	144 000	108 000	72 000
3D Matrix Dimension	2 000	16 000	16 000	16 000	30 000	30 000	30 000
ω	0.0085	0.25	0.25	0.49	0.2	0.08	0.1
npt2	20	60	60	80	80	60	40
α		0	1	1	1	1	1
Energy Threshold	45 000	45 000	45 000	45 000	200 000	200 000	200 000
zquad2	true	true	false	false	false	false	false
	2349.11514392	−226 888.88	24 374 226	4 005 386	2337	18	−4
	3612.84180777	−191 765.24	10 372 409	2 351 531	2765	146	82
	3714.78925087	−266 370.23	16 457 708	2 798 692	1489	95	76
	4853.63036539	−173 524.15	8 267 811	2 177 274	2970	169	123
	4977.84560897	−224 580.06	22 198 787	5 057 017	4852	121	50
	5099.67173901	−296 051.45	10 250 846	2 701 070	3171	214	145
	6075.98009595	−163 090.23	17 120 497	3 161 422	2920	184	162
	6227.92088226	−189 938.03	24 919 571	6 249 811	5351	197	119
	6347.87173516	−265 821.85	31 405 187	7 433 038	4766	147	127
	6503.09527395	−316 791.45	19 355 099	5 138 427	7790	327	201
	6972.56194714	−328 697.99	261 123.23	57 639 104	69 198	1206	−5
	7283.96483819	−154 729.63	32 998 988	5 207 467	2393	234	214
	7460.52277724	−168 809.84	35 397 808	6 945 089	6219	252	187
	7593.71247826	−227 515.60	44 349 230	143 811.0	39 570	200	120
	7734.46650916	−294 252.60	46 405 510	9 506 860	31 800	260	230
	7920.85399076	−335 374.60	47 941 060	9 845 100	16 510	410	280

is required in rovibrational $J > 0$ calculations, for which odd energy levels exist, and should thus be tested firstly for $J = 0$.

The initial joy of an excellent agreement between DVR3D Radau and Jacobi $J = 0$ even calculations was overshadowed by subsequent $J = 0$ odd calculations, which resulted in residuals of up to 2.5 cm^{-1} using the same basis set parameters. This issue has been previously encountered for H_3^+ [54] and is associated with the molecule encountering linear geometries.

Of course, CO_2 does have a linear equilibrium geometry, which means that the Jacobi coordinate r_2 is zero at equilibrium. The range of this coordinate is $0 \le r_2 < \infty$ with a boundary condition applying at $r_2 = 0$. The spherical oscillators we use are characterized by two parameters α and ω [18]; while these parameters are variational and can be optimized in the standard fashion, they also have a physical interpretation. ω corresponds to the frequency of vibration in the r_2 coordinate, while for harmonic solutions of the linear molecule problem

Table 5
A comparison of $J = 0$ even energy levels in units of cm^{-1} below 8 000 cm^{-1}. The digits in parentheses indicate deviations in the last two decimal places associated with the TROVE integration range.

E^{Radau}_{DVR3D}	$E^{Radau}_{EVEREST}$	E^{Radau}_{RV3}	E^{BLBA}_{TROVE}	$\Delta E^{Radau}_{EVEREST}$	ΔE^{Radau}_{RV3}	ΔE^{BLBA}_{TROVE}
1285.4143277	1285.4143290	1285.414340	1285.41436(06)	−0.0000013	−0.000012	−0.00003
1388.1865859	1388.1865874	1388.186602	1388.18662(06)	−0.0000015	−0.000016	−0.00003
2548.3661327	2548.3661348	2548.366159	2548.36626(13)	−0.0000021	−0.000026	−0.00013
2671.1396446	2671.1396466	2671.139663	2671.13955(08)	−0.0000020	−0.000018	0.00009
2797.1329921	2797.1329948	2797.133029	2797.13316(16)	−0.0000027	−0.000037	−0.00017
3792.6789375	3792.6789405	3792.678980	3792.67916(21)	−0.0000030	−0.000043	−0.00022
3942.5214837	3942.5214869	3942.521514	3942.52137(13)	−0.0000032	−0.000030	0.00011
4064.2621231	4064.2621266	4064.262160	4064.26208(15)	−0.0000035	−0.000037	0.00004
4225.0923366	4225.0923404	4225.092403	4225.09265(25)	−0.0000038	−0.000066	−0.00031
4673.2992155	4673.2992193	4673.299307	4673.29862(01)	−0.0000038	−0.000092	0.00060
5022.3600905	5022.3600946	5022.360143	5022.36040(28)	−0.0000041	−0.000052	−0.00031
5197.2334395	5197.2334440	5197.233480	5197.23340(20)	−0.0000045	−0.000041	0.00004
5329.6248353	5329.6248395	5329.624878	5329.62460(16)	−0.0000042	−0.000043	0.00024
5475.5398395	5475.5398445	5475.539903	5475.53995(25)	−0.0000050	−0.000063	−0.00011
5667.6395553	5667.6395606	5667.639646	5667.64001(35)	−0.0000053	−0.000091	−0.00045
5915.2050126	5915.2050179	5915.205112	5915.20446(06)	−0.0000053	−0.000099	0.00055
6016.7036775	6016.7036829	6016.703785	6016.70307(05)	−0.0000054	−0.000108	0.00061
6240.0950315	6240.0950365	6240.095099	6240.09542(35)	−0.0000050	−0.000068	−0.00039
6435.5146069	6435.5146120	6435.514665	6435.51466(27)	−0.0000051	−0.000058	−0.00005
6588.3180998	6588.3181048	6588.318139	6588.31778(19)	−0.0000050	−0.000039	0.00032
6725.2607286	6725.2607340	6725.260785	6725.26059(24)	−0.0000054	−0.000056	0.00014
6903.9118771	6903.9118830	6903.911964	6903.91214(35)	−0.0000059	−0.000087	−0.00026
7121.7212249	7121.7212316	7121.721340	7121.72182(45)	−0.0000067	−0.000115	−0.00060
7133.8056060	7133.8056121	7133.805719	7133.80514(13)	−0.0000061	−0.000113	0.00047
7259.7733518	7259.7733578	7259.773457	7259.77261(07)	−0.0000060	−0.000105	0.00074
7377.7145753	7377.7145820	7377.714699	7377.71406(13)	−0.0000067	−0.000124	0.00052
7447.7048515	7447.7048572	7447.704931	7447.70532(42)	−0.0000057	−0.000080	−0.00047
7659.9775932	7659.9775988	7659.977662	7659.97773(35)	−0.0000056	−0.000069	−0.00014
7834.8461947	7834.8462008	7834.846247	7834.84591(25)	−0.0000061	−0.000052	0.00028
7974.4251350	7974.4251414	7974.425183	7974.42475(24)	−0.0000064	−0.000048	0.00039

Table 6
A comparison of $J = 0$ odd energy levels in units of cm^{-1} below 8 000 cm^{-1}. The digits in parentheses indicate deviations in the last two decimal places associated with the TROVE integration range.

E^{Radau}_{DVR3D}	$E^{Radau}_{EVEREST}$	E^{Radau}_{RV3}	E^{BLBA}_{TROVE}	$\Delta E^{Radau}_{EVEREST}$	ΔE^{Radau}_{RV3}	ΔE^{BLBA}_{TROVE}
2349.1151439	2349.1151458	2349.115190	2349.11484(01)	−0.0000019	−0.000046	0.00030
3612.8418078	3612.8418111	3612.841864	3612.84155(06)	−0.0000033	−0.000056	0.00026
3714.7892509	3714.7892543	3714.789311	3714.78896(06)	−0.0000034	−0.000060	0.00029
4853.6303654	4853.6303695	4853.630438	4853.63019(13)	−0.0000041	−0.000073	0.00018
4977.8456090	4977.8456129	4977.845670	4977.84519(08)	−0.0000039	−0.000061	0.00042
5099.6717390	5099.6717437	5099.671820	5099.67156(14)	−0.0000047	−0.000081	0.00018
6075.9800960	6075.9801009	6075.980183	6075.98001(20)	−0.0000049	−0.000087	0.00009
6227.9208823	6227.9208875	6227.920956	6227.92045(13)	−0.0000052	−0.000074	0.00043
6347.8717352	6347.8717406	6347.871819	6347.87132(14)	−0.0000054	−0.000084	0.00042
6503.0952740	6503.0952798	6503.095383	6503.09523(24)	−0.0000058	−0.000109	0.00004
6972.5619471	6972.5619531	6972.562080	6972.56106(01)	−0.0000060	−0.000133	0.00089
7283.9648382	7283.9648442	7283.964935	7283.96483(27)	−0.0000060	−0.000097	0.00001
7460.5227772	7460.5227837	7460.522869	7460.52241(20)	−0.0000065	−0.000092	0.00037
7593.7124783	7593.7124844	7593.712567	7593.71186(15)	−0.0000061	−0.000089	0.00062
7734.4665092	7734.4665162	7734.466619	7734.46623(23)	−0.0000070	−0.000110	0.00028
7920.8539908	7920.8539981	7920.854127	7920.85408(33)	−0.0000073	−0.000136	−0.00009

α equals ℓ, the bending mode vibrational angular momentum [52]. For even calculations, the wavefunction can be finite at $r_2 = 0$, but must have a zero derivative such that it is symmetric about $r_2 = 0$; spherical oscillator functions with $\alpha = 0$ satisfy these conditions. Conversely, the wavefunction of odd functions must be zero at $r_2 = 0$, but can have a finite derivative such that it is anti-symmetric about $r_2 = 0$; spherical oscillator functions with $\alpha = 1$ satisfy these conditions.

In short, for odd calculations, the α parameter must be changed from zero to unity. Additionally, integrals involving r_2^{-2} must be evaluated analytically instead of using the quadrature approximation [55]. Through careful optimization of the basis set size, as summarized in Table 3, and increase of the total matrix dimension, as presented in Table 4, agreement between DVR3D Radau and Jacobi calculations was achieved. This demonstrates that a wide range of parameters allows for good convergence in the even Jacobi calculations, while only a narrow range is permitted for odd Jacobi calculations. We note that in Radau coordinates there is no differential convergence between the two symmetries as there are no physically important geometries with $r_2 = 0$.

As shown in Table 4, the standard deviation of the difference between the best converged Jacobi and Radau coordinate calculations is 1.5×10^{-6} cm^{-1} for all levels up to 8 000 cm^{-1}. However, for two levels the difference is less than 10^{-6} cm^{-1}, which, in more convenient units, is less than 30 kHz. As the calculated Jacobi levels are almost always a little higher in energy, this suggests that the levels calculated in Radau coordinates are converged to about 3 kHz.

Input files for DVR3D for calculations with both $J = 0$ and $J = 20$ are given in the supplementary material to aid reproducibility.

4. Energy level calculations with other programs

This section presents $J = 0$ and $J = 20$ energy levels for EVEREST, RV3 and TROVE in comparison to those calculated using DVR3D with

Table 7
A comparison of $J = 20$ even e energy levels below 6 000 cm^{-1}.

E^{Radau}_{DVR3D}	E^{Jacobi}_{DVR3D}	$E^{Radau}_{EVEREST}$	E^{Radau}_{RV3}	E^{BLBA}_{TROVE}	$\Delta E^{Jacobi}_{DVR3D}$	$\Delta E^{Radau}_{EVEREST}$	ΔE^{Radau}_{RV3}	ΔE^{BLBA}_{TROVE}
163.8690129	163.8690129	163.8690129	163.8690167	163.868967	0.0000000	0.0000000	−0.0000038	0.000046
1449.3898110	1449.3898118	1449.3898123	1449.3898255	1449.389795	−0.0000008	−0.0000013	−0.0000145	0.000016
1499.5901561	1499.5901567	1499.5901568	1499.5901840	1499.589730	−0.0000006	−0.0000007	−0.0000279	0.000426
1552.0457834	1552.0457843	1552.0457849	1552.0458015	1552.045774	−0.0000009	−0.0000015	−0.0000181	0.000009
2712.6006761	2712.6006774	2712.6006783	2712.6007055	2712.600751	−0.0000013	−0.0000022	−0.0000294	−0.000075
2749.6085894	2749.6085896	2749.6085903	2749.6086265	2749.607995	−0.0000002	−0.0000009	−0.0000371	0.000594
2834.7320649	2834.7320654	2834.7320668	2834.7320866	2834.731924	−0.0000005	−0.0000019	−0.0000217	0.000141
2836.7649242	2836.7649240	2836.7649244	2836.7649758	2836.764331	0.0000002	−0.0000002	−0.0000516	0.000593
2925.1414858	2925.1414861	2925.1414870	2925.1415311	2925.140862	−0.0000003	−0.0000012	−0.0000453	0.000624
2961.1705389	2961.1705405	2961.1705416	2961.1705782	2961.170661	−0.0000016	−0.0000027	−0.0000393	−0.000122
3166.7758464	3166.7758506	3166.7758526	3166.7759143	3166.775008	−0.0000042	−0.0000062	−0.0000679	0.000838
3957.1841942	3957.1841958	3957.1841972	3957.1842351	3957.184362	−0.0000016	−0.0000030	−0.0000409	−0.000168
3986.7739850	3986.7739856	3986.7739869	3986.7740301	3986.773225	−0.0000006	−0.0000019	−0.0000451	0.000760
4063.4966323	4063.4966323	4063.4966333	4063.4966919	4063.495875	0.0000000	−0.0000010	−0.0000596	0.000757
4106.1201338	4106.1201350	4106.1201371	4106.1201657	4106.119973	−0.0000012	−0.0000033	−0.0000319	0.000161
4172.2829649	4172.2829661	4172.2829676	4172.2830185	4172.282165	−0.0000012	−0.0000027	−0.0000536	0.000800
4175.3203522	4175.3203519	4175.3203526	4175.3204274	4175.319592	0.0000003	−0.0000004	−0.0000752	0.000760
4227.8742738	4227.8742752	4227.8742773	4227.8743104	4227.874187	−0.0000014	−0.0000035	−0.0000366	0.000087
4287.2502218	4287.2502219	4287.2502230	4287.2502913	4287.249428	−0.0000001	−0.0000012	−0.0000695	0.000794
4361.7972245	4361.7972253	4361.7972269	4361.7972894	4361.796404	−0.0000008	−0.0000024	−0.0000649	0.000821
4389.2946701	4389.2946722	4389.2946740	4389.2947339	4389.294937	−0.0000021	−0.0000039	−0.0000638	−0.000267
4410.5582371	4410.5582470	4410.5582496	4410.5583161	4410.557135	−0.0000099	−0.0000125	−0.0000790	0.001102
4478.4349346	4478.4349348	4478.4349370	4478.4350173	4478.434141	−0.0000002	−0.0000024	−0.0000827	0.000794
4553.3047514	4553.3047615	4553.3047642	4553.3048387	4553.303611	−0.0000101	−0.0000128	−0.0000873	0.001140
4834.5826178	4834.5826177	4834.5826217	4834.5827188	4834.581974	0.0000001	−0.0000039	−0.0001010	0.000644
5187.1168607	5187.1168629	5187.1168648	5187.1169101	5187.117116	−0.0000022	−0.0000041	−0.0000494	−0.000255
5212.2345777	5212.2345787	5212.2345805	5212.2346304	5212.233653	−0.0000010	−0.0000028	−0.0000527	0.000925
5280.8561836	5280.8561840	5280.8561855	5280.8562507	5280.855263	−0.0000004	−0.0000019	−0.0000671	0.000921
5361.0452202	5361.0452220	5361.0452246	5361.0452617	5361.045128	−0.0000018	−0.0000044	−0.0000415	0.000092
5383.9500044	5383.9500041	5383.9500054	5383.9500909	5383.949083	0.0000003	−0.0000010	−0.0000865	0.000921
5409.8665416	5409.8665426	5409.8665448	5409.8666003	5409.865563	−0.0000010	−0.0000032	−0.0000587	0.000979
5492.8642056	5492.8642069	5492.8642099	5492.8642439	5492.863923	−0.0000013	−0.0000043	−0.0000383	0.000283
5510.9708253	5510.9708256	5510.9708275	5510.9709095	5510.969860	−0.0000003	−0.0000022	−0.0000842	0.000965
5515.1822406	5515.1822404	5515.1822415	5515.1823417	5515.181322	0.0000002	−0.0000009	−0.0001011	0.000919
5601.4644768	5601.4644778	5601.4644802	5601.4645479	5601.463469	−0.0000010	−0.0000034	−0.0000711	0.001008
5637.9579871	5637.9580023	5637.9580053	5637.9580798	5637.956711	−0.0000152	−0.0000182	−0.0000927	0.001276
5639.4722310	5639.4722343	5639.4722370	5639.4722963	5639.472196	−0.0000033	−0.0000060	−0.0000653	0.000035
5645.3267489	5645.3267486	5645.3267502	5645.3268470	5645.325786	0.0000003	−0.0000013	−0.0000981	0.000963
5694.9687877	5694.9687887	5694.9687915	5694.9688830	5694.967827	−0.0000010	−0.0000038	−0.0000953	0.000961
5745.0706710	5745.0706715	5745.0706735	5745.0707644	5745.069676	−0.0000005	−0.0000025	−0.0000934	0.000995
5791.4424276	5791.4424276	5791.4424301	5791.4425334	5791.441473	0.0000000	−0.0000025	−0.0001058	0.000955
5795.2941155	5795.2941287	5795.2941322	5795.2942099	5795.292731	−0.0000132	−0.0000167	−0.0000944	0.001385
5809.3289357	5809.3289370	5809.3289394	5809.3290206	5809.327917	−0.0000013	−0.0000037	−0.0000849	0.001019
5831.9737256	5831.9737285	5831.9737309	5831.9738110	5831.974137	−0.0000029	−0.0000053	−0.0000854	−0.000411
5894.0719751	5894.0719762	5894.0719792	5894.0720802	5894.070981	−0.0000011	−0.0000041	−0.0001051	0.000994

Radau coordinates. The residuals are calculated as the signed difference between DVR3D Radau and the other program ($\Delta E = E^{Radau}_{DVR3D} - E_{other}$).

EVEREST (Electronic, Vibrational Et Rotational Energies and Spectra for Triatomics) [22] calculates rovibronic energies, wavefunctions and dipole transition moments for triatomic molecules. The procedure employed is analogous to DVR3D, however, any number of electronic states with arbitrary couplings (*e.g.* spin–orbit and non-adiabatic) and Renner–Teller effects can be treated. It also supports the use of sinc-DVR basis functions for radial degrees of freedom. In this work, EVEREST calculations were performed in Radau coordinates using a bisector embedding; the calculations used 60 sinc-DVR radial and 120 Legendre angular basis functions with a vibrational matrix dimension of 20 000. The rotational matrix was constructed with a maximum dimension of 50 000 using the lowest energy vibrational eigenfunctions allowed within each symmetry block.

RV3 [26,27] likewise calculates rovibrational energy levels, wavefunctions and intensities for a triatomic molecules using a variety of basis function types and embedding frames.

TROVE (Theoretical ROVibrational Energies) [56] calculates rovibrational energy levels and spectra for polyatomic molecules. It originally used an approximate kinetic energy operator for triatomic molec ules, however, an exact form has now been programmed [21]. Unlike DVR3D and EVEREST that define quadratures to evaluate associated integrals, TROVE uses the finite basis representation (FBR) with basis sets constructed as products of one-dimensional functions. The advantage of this approach is that all integrals involved in the evaluation of each Hamiltonian matrix element are numerically exact. This means that the Hamiltonian operator (*i.e.* both the kinetic energy operator and potential energy surface) must be represented as a sum of products, which is not always practical or possible. For a linear triatomic molecule such as CO_2, the bisector embedding is used in TROVE, which is known to produce the exact form of the kinetic energy operator (KEO) in the sum-of-products form [57]. While TROVE's KEO is in the sum-of-products form by construction, potential functions, often do not have the required form and require additional re-expansions, usually as Taylor-series, which is never exact.

The calculations presented here use essentially the same set-up as in Yurchenko et al. [58], except for the integration range (see below).

The variational TROVE program [56] solves the ro-vibrational Schrödinger equation using a multi-layer contraction scheme (see, for example, Yurchenko et al. [59]) with the 1D primitive basis set functions obtained by numerically solving the corresponding Schrödinger equations. A 1D Hamiltonian operator for a given mode is constructed by setting all other degrees of freedom to their equilibrium values. The two equivalent stretching equations are solved on a grid of 1000 points using the Numerov-Cooley approach [60,61]. The bending mode solutions are obtained on the basis of the associated Laguerre polynomials. The kinetic energy operator is constructed numerically exact as

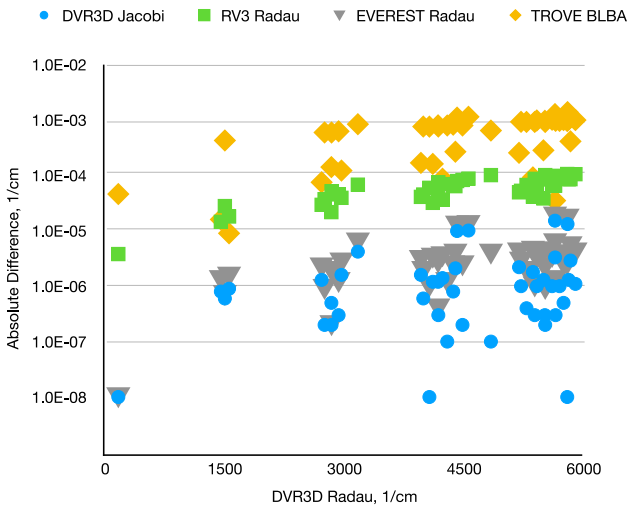

Fig. 1. The differences for $J = 20$ even e energy levels below 6 000 cm^{-1} (see Table 7) between the energies calculated using different programs.

a formal expansion in terms of the inverse powers of the stretching coordinates r_i ($i = 1, 2$): $1/r_i$ and $1/r_i^2$ around a non-rigid configuration [62] defined by the ρ_i points on the grid. In order to be compatible with the TROVE internal coordinates, the PES Ames-2 of CO_2 used here had to be re-expanded around the non-rigid configuration in terms of powers of $1-\exp(-(r-r_e))$ up to 14th order. Here, $r_e = 1.1613997389$ Å is the equilibrium parameter as defined by the AMES-2 function. This re-expansion is arguably the main source of the discrepancy between TROVE and other codes (see below).

An $E = hc \times 36\,000$ cm^{-1} energy cut-off was used to contract the $J = 0$ eigenfunctions. The size of the vibrational basis was controlled by a polyad-number condition:

$$P = v_1 + v_2 + v_3 \le P_{\max} = 64,$$

chosen based on the convergence tests with v_1 and $v_2 \le 52$.

In TROVE calculations, the ro-vibrational states are uniquely identified by three numbers, the rotational angular momentum quantum number J, the total symmetry Γ (Molecular symmetry group) and the eigenstate counting number λ (in the order of increasing energies). Each state can be further assigned with approximate quantum numbers (QN) associated with the corresponding largest basis set contribution [56].

4.1. $J = 0$ and $J = 20$ calculations

Tables 5 and 6 present $J = 0$ energy levels below 8 000 cm^{-1} computed with the aforementioned programs for even and odd calculations, respectively. Table 7 and Fig. 1 present $J = 20$ energy levels in units of cm^{-1} below 6 000 cm^{-1} for the even e calculations and differences between their values calculated using different programs. A further comparison for $J = 0$ between the DVR3D Radau calculations and those of Huang et al. [35] is given in the supplementary material. Although the agreement is very good, better than 10^{-3} cm^{-1} in all cases, but we cannot be certain about the precision of the values of constants used in these calculations.

The agreement encountered for all programs is exceptional. In comparison to DVR3D Radau calculations, the discrepancy is on the order of $10^{-6} - 10^{-5}$ cm^{-1} for EVEREST, $10^{-5} - 10^{-4}$ cm^{-1} for RV3, and $10^{-4} - 10^{-3}$ cm^{-1} for TROVE, respectively. The agreement for high $J = 20$ calculations is not significantly worse than that for $J = 0$, which is reassuring for high-temperature line list production in the study of exoplanet and other hot atmospheres [63].

4.2. Discussion

EVEREST agrees best with the DVR3D Radau $J = 0$ and $J = 20$ calculations, which may be due to similarities in overall program structure. The apparent linear drift in the residuals was not explored further, however, it is likely due to the diagonalization routine employed in each code. Nevertheless, the discrepancies on the order of $10^{-6} - 10^{-5}$ cm^{-1} are exceptional for two independent programs converged with different basis sets. This agreement using the sinc-DVR implementation in EVEREST is thus further promising for applications to photodissociation [64]; the control of the radial box size [65] allows for a robust treatment of long bond length behavior as the basis completely spans the chosen grid [66]. This is compromised by the larger matrix dimensions required for convergence to high accuracy in comparison to Morse-like oscillator functions, which conversely require careful molecule-specific optimization to be efficient.

TROVE yields the largest discrepancy with respect to the other programs, almost certainly due to the re-expansion of the potential energy surface. This is because the Ames-2 CO_2 PES is not represented as a simple sum-of-products of one-dimensional components [35]. This approach breaks the exact numerical equivalence between the original Ames-2 PES used directly by the other programs, although the observed error is well below 10^{-3} cm^{-1}. The main parameter affecting the accuracy in the re-expansion was the integration range along the bending coordinate θ_{OCO}. Our calculations used $\theta_{OCO} \in [180° \ldots 75°]$, which produced the closest match with the DVR3D energy levels. Tables 5 and 6 indicate deviations in the last two decimal places associated with the TROVE integration range for $J = 0$ calculations.

Finally, while the focus of this paper is solving the CO_2 rotation–vibration problem as posed to a given accuracy using a number of different codes, it is also of interest to compare the calculated results with experiment. The supplementary data gives a comparison between the DVR3D Radau calculations and the empirical energy levels of $^{12}C^{16}O_2$ obtained as a part of a recent MARVEL study [34]. While it can be seen that the agreement is good, generally 0.02 cm^{-1} or better, it is worse than the general convergence of the calculations. This suggests that further improvements will have to be achieved by improving the model parameters, such as the accuracy of the potential energy surface used, rather than the accuracy, with which the nuclear motion problem is solved.

5. Intensity calculations

A key assessment of the high-accuracy solution of the rovibrational Schrödinger equation is the corresponding intensity results. An absolute accuracy of 10^{-6} cm^{-1} in the energy levels corresponds to a relative accuracy better than 10^{-9}. It was therefore predicted that the corresponding Einstein A coefficients should give rise to the same relative accuracy as the corresponding dipole matrix elements are calculated from the same high-accuracy wavefunctions.

Table 8 and Fig. 2 present Einstein A coefficients for selected R(2) and P(3) transitions calculated in the aforementioned programs, along with the associated HITRAN values [33] collated from [44,67,68].

The intensity calculations in DVR3D can only be performed within the same (even/odd) symmetry block. It was thus necessary to perform both Radau and Jacobi calculations here with $\alpha = 0$ even wavefunctions. This change in basis functions lead to a shift in the odd Jacobi energy levels of 0.1 – 0.7 cm^{-1}, which is a decrease in accuracy by five orders of magnitude. Therefore, the accuracy of the intensity calculations is also expected deteriorate. Table 8 shows that between DVR3D Radau and Jacobi calculations, most Einstein A coefficients coincide reasonably well, whereas some differ by one to two orders of magnitude. This comparison illustrates the issue that one has to be very careful with the use of Jacobi coordinates in intensity calculations for (quasi-)linear molecules, as they can give large differences in Einstein A coefficients even when differences in energy levels are relatively small.

Table 8
A comparison of Einstein A coefficients for selected R(2) and P(3) transitions in units of s^{-1} for DVR3D and EVEREST. The final column indicates the source of the HITRAN Einstein A coefficient.

Upper assignment	Lower assignment	ν MARVEL	ν DVR3D Jacobi	ν DVR3D Radau	A DVR3D Jacobi	A DVR3D Radau	A EVEREST Radau	A HITRAN	
(2 2 0 0 0 3 e)	(3 0 0 0 1 1 e)	196.923	196.041	196.952	4.253E−06	4.528E−06	4.644E−06	4.478E−06	[44]
(2 2 0 0 0 3 e)	(3 1 1 1 0 1 e)	469.171	468.749	469.178	2.106E−03	2.010E−03	2.025E−03	2.006E−03	[44]
(2 2 0 0 0 3 e)	(3 0 3 3 0 1 e)	542.757	542.772	542.779	1.052E−09	1.059E−09	1.061E−09	–	–
(3 1 1 1 0 2 e)	(2 1 0 0 0 1 e)	546.634	546.979	546.630	1.900E−02	1.919E−02	1.921E−02	1.920E−02	[44]
(3 1 1 1 0 2 e)	(2 0 2 2 0 1 e)	599.678	600.043	599.694	2.703E−02	2.729E−02	2.741E−02	2.730E−02	[44]
(2 2 0 0 0 3 e)	(3 1 1 1 0 2 e)	613.552	613.206	613.555	1.110E+00	1.089E+00	1.095E+00	1.089E+00	[44]
(2 1 0 0 0 2 e)	(3 0 1 1 0 1 e)	615.684	615.441	615.701	5.075E−01	4.982E−01	5.012E−01	4.983E−01	[44]
(3 0 3 3 0 1 e)	(2 1 0 0 0 1 e)	617.429	617.413	617.406	1.006E−09	9.795E−10	9.848E−10	–	–
(3 1 1 1 0 2 e)	(2 1 0 0 0 2 e)	649.408	649.749	649.401	1.182E+00	1.180E+00	1.183E+00	1.180E+00	[44]
(2 0 2 2 0 1 e)	(3 0 1 1 0 1 e)	665.414	665.148	665.407	2.040E−01	1.984E−01	1.992E−01	1.985E−01	[44]
(3 0 1 1 0 1 e)	(2 0 0 0 0 1 e)	669.726	669.974	669.715	8.885E−01	8.870E−01	8.892E−01	8.869E−01	[44]
(3 0 3 3 0 1 e)	(2 0 2 2 0 1 e)	670.473	670.477	670.470	3.296E+00	3.266E+00	3.279E+00	3.266E+00	[44]
(3 1 1 1 0 1 e)	(2 1 0 0 0 1 e)	691.015	691.436	691.007	1.370E+00	1.364E+00	1.367E+00	1.363E+00	[44]
(2 1 0 0 0 1 e)	(3 0 1 1 0 1 e)	718.458	718.212	718.471	7.163E−01	6.998E−01	7.043E−01	6.997E−01	[44]
(3 0 3 3 0 1 e)	(2 1 0 0 0 2 e)	720.203	720.184	720.177	1.879E−09	1.857E−09	1.868E−09	–	–
(3 1 1 1 0 1 e)	(2 0 2 2 0 1 e)	744.059	744.500	744.071	4.616E−02	4.608E−02	4.630E−02	4.606E−02	[44]
(3 1 1 1 0 1 e)	(2 1 0 0 0 2 e)	793.790	794.206	793.777	6.043E−02	5.895E−02	5.907E−02	5.893E−02	[44]
(3 0 0 0 1 1 e)	(2 1 0 0 0 1 e)	963.263	964.144	963.233	1.779E−01	1.686E−01	1.670E−01	1.680E−01	[44]
(3 0 0 0 1 1 e)	(2 0 2 2 0 1 e)	1016.307	1017.208	1016.297	1.594E−08	3.192E−09	2.869E−09	–	–
(3 0 0 0 1 1 e)	(2 1 0 0 0 2 e)	1066.037	1066.915	1066.004	1.968E−01	1.879E−01	1.893E−01	1.872E−01	[44]
(2 2 0 0 0 3 e)	(3 0 1 1 0 1 e)	1878.644	1878.397	1878.656	3.584E−06	9.354E−05	3.717E−05	9.740E−05	[67]
(3 1 1 1 0 2 e)	(2 0 0 0 0 1 e)	1934.818	1935.165	1934.817	2.812E−04	1.848E−04	2.940E−04	2.008E−04	[68]
(3 0 3 3 0 1 e)	(2 0 0 0 0 1 e)	2005.613	2005.600	2005.593	1.035E−11	7.634E−12	7.688E−12	–	–
(3 0 3 3 0 1 e)	(2 0 0 0 0 1 e)	2079.199	2079.622	2079.193	4.439E−03	3.227E−03	2.736E−03	3.229E−03	[44]
(3 0 0 0 1 1 e)	(2 0 0 0 0 1 e)	2351.447	2352.331	2351.419	1.854E+02	1.811E+02	1.809E+02	1.811E+02	[44]

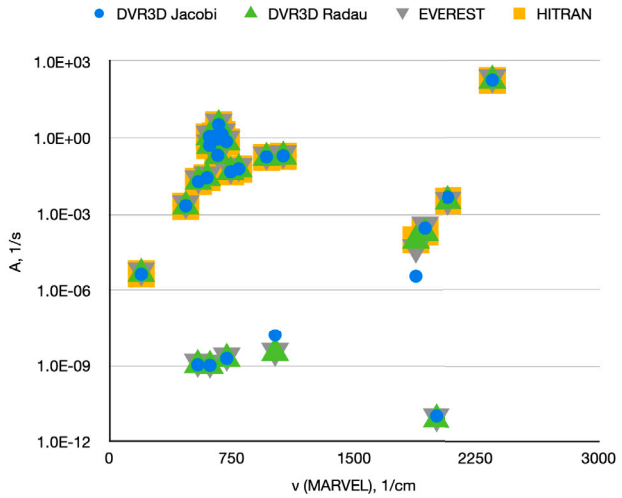

Fig. 2. A comparison of Einstein A coefficients for selected R(2) and P(3) transitions for DVR3D, EVEREST, and HITRAN (see Table 8).

Recent studies [53,69] have shown similarly that Radau coordinates are preferable for intensity calculations on the asymmetric linear molecule N_2O.

The Einstein A coefficients from HITRAN in Table 8 are predominately derived from the theoretical study of Zak et al. [44]. These *ab initio* line intensities were calculated in DVR3D using Radau coordinates with older Ames surfaces [13,70]. This study also identified 'sensitive' bands using the Lodi-Tennyson method [71], which are influenced by strong resonance interactions and thus involve greater uncertainty in line intensity calculations. Consequently, the excellent agreement between the HITRAN results and the current DVR3D Radau results is unsurprising. For the lines at 1878.644 and 1934.818 cm^{-1}, CDSD [67,68] Einstein A coefficients were preferred for inclusion in HITRAN following use of the aforementioned resonance identification procedure. This explains the greater discrepancy across programs for these two lines. The comparison between the DVR3D Radau and EVEREST intensity calculations is satisfactory. The majority of transitions exhibit sub-percent agreement, however, there are several lines with 10 – 60% error, notably for the two lines identified to be associated with resonance energy levels.

6. Conclusion

Achievements in rovibrational experimental and theoretical studies are very much linked. Recent significant increases in the accuracy of the near-infrared experimental line positions, determined to kHz accuracy [5] (which corresponds to better than 12 figure accuracy) and the improved accuracy of the intensity measurements, to about 0.1% [6], demand corresponding theoretical improvements in the first principles variational calculations. In this paper, we demonstrate that variational nuclear motion calculations can compute energy levels with an accuracy as little as 10 kHz for the benchmark triatomic CO_2.

The agreement for the transition intensities, represented by Einstein A coefficients and computed using the various programs, is satisfactory. There are issues with lines involving levels, which are known to be involved in resonance interactions, plus the previously documented issue with treating a linear molecule such as CO_2 in Jacobi coordinates [69]. It would appear that little more work is required to bring these codes into agreement at the permille level now being achieved experimentally.

Our results in general point to new possibilities. First, it would be interesting to expand our results to other important triatomic molecules, such as water, ozone, N_2O and HCN; tests with a non-linear molecule would be particularly important as many could yield somewhat different results. Second, the accuracy to which energy levels can be computed opens the way towards much better fits for the PESs of CO_2 and other important triatomic molecules to experimentally derived energy levels; hopefully, these can achieve accuracies close to 10^{-3} cm^{-1}, which corresponds to the accuracy of the experimentally levels using Fourier Transform Spectrometers, and perhaps also towards kHz level of accuracy for PESs when based on energy levels, for which this accuracy has been achieved using laser spectrometers [1–3]. A third direction would be the comparison of our results with all other

triatomic nuclear motion programs in current use and extending the comparisons to consider rovibronic transitions and the inclusion of Renner–Teller interactions.

CRediT authorship contribution statement

Roman I. Ovsyannikov: Writing – review & editing, Methodology, Formal analysis. **Armando N. Perri:** Writing – review & editing, Validation, Methodology, Investigation, Formal analysis, Data curation. **Irina I. Mizus:** Visualization, Investigation. **Jonathan Tennyson:** Writing – review & editing, Supervision, Software, Methodology. **Sergei N. Yurchenko:** Software, Investigation. **Alexander O. Mitrushchenkov:** Software, Investigation. **Nikolai F. Zobov:** Writing – review & editing, Methodology, Investigation, Formal analysis. **Mikhail A. Rogov:** Investigation. **Oleg L. Polyansky:** Writing – review & editing, Supervision, Project administration, Methodology, Investigation, Formal analysis, Conceptualization.

Declaration of competing interest

The authors declare that they have no known competing financial interests or personal relationships that could have appeared to influence the work reported in this paper.

Acknowledgments

This work is supported by State Project IAP RAS No. FFUF-2024-0016. The authors are grateful to Xiaogang Wang and Tucker Carrington for useful comments and discussion. This work was also supported by the European Research Council (ERC) under the European Union's Horizon 2020 research and innovation programme through Advance Grant number 883830, and STFC, United Kingdom projects ST/Y001508/1 and UKRI/ST/B001183/1.

Appendix A. Supplementary data

Supplementary material related to this article can be found online at https://doi.org/10.1016/j.jms.2025.112068.

Data availability

Data are contained within the article and the supporting material.

References

[1] S. Jiang, Y. Tan, A.-W. Liu, X.-G. Zhou, S.-M. Hu, Saturated cavity ring-down spectroscopy of $^{12}C^{16}O_2$ near 1.57μm, Chin. J. Chem. Phys. 37 (2024) 13–18, http://dx.doi.org/10.1063/1674-0068/cjcp2305046.

[2] H. Wu, C.-L. Hu, J. Wang, Y.R. Sun, Y. Tan, A.-W. Liu, S.-M. Huab, A well-isolated vibrational state of CO_2 verified by near-infrared saturated spectroscopy with khz accuracy, Phys. Chem. Chem. Phys. 22 (2020) 2841–2848, http://dx.doi.org/10.1039/C9CP05121J.

[3] Y. Tan, Y.-R. Xu, T.-P. Hua, A.-W. Liu, J. Wang, Y.R. Sun, S.-M. Hu, Cavity-enhanced saturated absorption spectroscopy of the (30012) – (00001) band of $^{12}C^{16}O_2$, J. Chem. Phys. 156 (2022) 044201, http://dx.doi.org/10.1063/5.0074713.

[4] S.N. Mikhailenko, E.V. Karlovets, A.O. Koroleva, A. Campargue, The far-infrared absorption spectrum of $HD^{16}O$: Experimental line positions, accurate empirical energy levels, and a recommended line list, Molecules 29 (2024) 5508, http://dx.doi.org/10.3390/molecules29235508.

[5] J. Wang, C.-L. Hu, A.-W. Liu, Y. Sun, Y. Tan, S.-M. Hu, Saturated absorption spectroscopy near 1.57μm and revised rotational line list of $^{12}C^{16}O$, J. Quant. Spectrosc. Radiat. Transfer 270 (2021) 107717, http://dx.doi.org/10.1016/j.jqsrt.2021.107717.

[6] K. Bielska, A.A. Kyuberis, Z.D. Reed, G. Li, A. Cygan, R. Ciurył o, E.M. Adkins, L. Lodi, N.F. Zobov, V. Ebert, D. Lisak, J.T. Hodges, J. Tennyson, O.L. Polyansky, Subpromille Measurements and Calculations of CO (3–0) Overtone Line Intensities, Phys. Rev. Lett. 129 (2022) 043002, http://dx.doi.org/10.1103/PhysRevLett.129.043002.

[7] A.A. Balashov, K. Bielska, G. Li, A.A. Kyuberis, S. Wójtewicz, J. Domysławska, R. Ciuryło, N.F. Zobov, D. Lisak, J. Tennyson, O.L. Polyansky, Measurement and calculation of CO (7–0) overtone line intensities, J. Chem. Phys. 158 (2023) 234306, http://dx.doi.org/10.1063/5.0152996.

[8] D.A. Long, Z.D. Reed, A.J. Fleisher, J. Mendonca, S. Roche, J.T. Hodges, High-accuracy near-infrared carbon dioxide intensity measurements to support remote sensing, Geophys. Res. Lett. 47 (e2019GL086344) (2020) http://dx.doi.org/10.1029/2019GL086344, e2019GL086344.

[9] J.T. Hodges, K. Bielska, M. Birk, R. Guo, G. Li, J.S. Lim, D. Lisak, Z.D. Reed, G. Wagner, International comparison ccqm-p229 pilot study to measure line intensities of selected $^{12}C^{16}O$ transitions, Metrologia 62 (2025) 08006, http://dx.doi.org/10.1088/0026-1394/62/1A/08006.

[10] J.-K. Li, J. Wang, R.-H. Yin, Q. Huang, Y. Tan, C.-L. Hu, Y.R. Sun, O.L. Polyansky, N.F. Zobov, E.I. Lebedev, R. Stosch, J. Tennyson, G. Li, S.-M. Hu, Unprecedented accuracy in molecular line-intensity ratios from frequency-based measurements, Sci. Adv. 11 (2025) http://dx.doi.org/10.1126/sciadv.adz6560, eadz6560.

[11] A.A.A. Azzam, S.A.A. Azzam, K.A.A. Aburumman, J. Tennyson, S.N. Yurchenko, A.G. Császár, T. Furtenbacher, MARVEL analysis of high-resolution rovibrational spectra of $^{18}O^{12}C^{18}O$, $^{17}O^{12}C^{18}O$ and $^{18}O^{13}C^{18}O$ isotopologues of carbon dioxide, J. Mol. Spectrosc. 405 (2024) 111947, http://dx.doi.org/10.1016/j.jms.2024.111947.

[12] A.A.A. Azzam, J.M.A. AlAlawin, J. Tennyson, S.N. Yurchenko, T. Furtenbacher, A.G. Császár, MARVEL analysis of high-resolution rovibrational spectra of $^{17}O^{13}C^{18}O$ and $^{17}O^{13}C^{17}O$, J. Quant. Spectrosc. Radiat. Transfer 343 (2025) 109485, http://dx.doi.org/10.1016/j.jqsrt.2025.109485.

[13] X. Huang, D.W. Schwenke, S.A. Tashkun, T.J. Lee, An isotopic-independent highly accurate potential energy surface for CO_2 isotopologues and an initial $^{12}C^{16}O_2$ infrared line list, J. Chem. Phys. 136 (2012) 124311, http://dx.doi.org/10.1063/1.3697540.

[14] S.N. Yurchenko, L. Lodi, J. Tennyson, A.V. Stolyarov, DUO: a general program for calculating spectra of diatomic molecules, Comput. Phys. Comm. 202 (2016) 262–275, http://dx.doi.org/10.1016/j.cpc.2015.12.021.

[15] R.J. Le Roy, LEVEL: A Computer Program for Solving the Radial Schrödinger Equation for Bound and Quasibound Levels, J. Quant. Spectrosc. Radiat. Transfer 186 (2017) 167–178, http://dx.doi.org/10.1016/j.jqsrt.2016.05.028.

[16] I.I. Mizus, L. Lodi, J. Tennyson, N.F. Zobov, O.L. Polyansky, An analysis of the accuracy of line intensities calculations using DUO and LEVEL program package, J. Mol. Spectrosc. 386 (2022) 111621, http://dx.doi.org/10.1016/j.jms.2022.111621.

[17] N.F. Zobov, R.I. Ovsyannikov, M.A. Rogov, E.I. Lebedev, J. Tennyson, O.L. Polyansky, CO line intensities: Towards subpercent accuracy of intensities of all bands, J. Quant. Spectrosc. Radiat. Transfer 325 (2025) 109510, http://dx.doi.org/10.1016/j.jqsrt.2025.109510.

[18] J. Tennyson, M.A. Kostin, P. Barletta, G.J. Harris, O.L. Polyansky, J. Ramanlal, N.F. Zobov, DVR3D: a program suite for the calculation of rotation-vibration spectra of triatomic molecules, Comput. Phys. Comm. 163 (2004) 85–116.

[19] J. Tennyson, S. Miller, C.R. Le Sueur, TRIATOM: programs for the calculation of ro-vibrational spectra of triatomic molecules, Comput. Phys. Comm. 75 (1993) 339–364.

[20] S.N. Yurchenko, W. Thiel, P. Jensen, Theoretical ROVibrational energies (TROVE): A robust numerical approach to the calculation of rovibrational energies for polyatomic molecules, J. Mol. Spectrosc. 245 (2007) 126–140, http://dx.doi.org/10.1016/j.jms.2007.07.009.

[21] S.N. Yurchenko, T.M. Mellor, Treating linear molecules in calculations of rotation vibration spectra, J. Chem. Phys. 153 (2020) 154106, http://dx.doi.org/10.1063/5.0019546.

[22] A.O. Mitrushchenkov, A new general Renner-Teller (including $\epsilon \geq 1$) spectroscopic formalism for triatomic molecules, J. Chem. Phys. 136 (2012) 024108, http://dx.doi.org/10.1063/1.3672162.

[23] D.W. Schwenke, Variational calculations of rovibrational energy levels and transition intensities for tetratomic molecules, J. Phys. Chem. 100 (1996) 2867–2884.

[24] J. Sarka, D. Das, B. Poirier, Calculation of rovibrational eigenstates of H_3^+ using scalit, AIP Adv. 11 (2021) 045033, http://dx.doi.org/10.1063/5.0047823.

[25] E. Mátyus, G. Czakó, B.T. Sutcliffe, A.G. Császár, Vibrational energy levels with arbitrary potentials using the Eckart-Watson Hamiltonians and the discrete variable representation, J. Chem. Phys. 127 (2007) 084102, http://dx.doi.org/10.1063/1.2756518.

[26] X.G. Wang, T. Carrington, RV3: A package of programs to compute rovi-brational levels and wavefunctions of triatomic molecules..

[27] X.-G. Wang, T. Carrington Jr., A two-step quadrature-based variational calculation of ro-vibrational levels and wavefunctions of CO_2 using a bisector-x body-fixed frame, Phys. Chem. Chem. Phys. 26 (2024) 15181, http://dx.doi.org/10.1039/D4CP00655K.

[28] D. Lauvergnat, A. Nauts, Exact numerical computation of a kinetic energy operator in curvilinear coordinates, J. Chem. Phys. 116 (2002) 8560–8570, http://dx.doi.org/10.1063/1.1469019.

[29] J.R. Henderson, S. Miller, J. Tennyson, Calculated ro-vibrational spectrum of $^7Li_3^+$ and $^7Li_2^6Li^+$, Spectrochim. Acta 44A (1988) 1287–1290.

[30] S. Carter, P. Rosmus, N.C. Handy, S. Miller, J. Tennyson, B.T. Sutcliffe, Benchmark calculations of first principles rotational and ro-vibrational line strengths, Comput. Phys. Comm. 55 (1989) 71–75.

[31] O.L. Polyansky, A.G. Császár, S.V. Shirin, N.F. Zobov, P. Barletta, J. Tennyson, D.W. Schwenke, P.J. Knowles, High accuracy ab initio rotation-vibration transitions of water, Science 299 (2003) 539–542.

[32] C.A. Bowesman, I.I. Mizus, N.F. Zobov, O.L. Polyansky, J. Sarka, B. Poirier, M. Pezzella, S.N. Yurchenko, J. Tennyson, ExoMol line lists - l: High-resolution line lists of H_3^+, H_2D^+, D_2H^+ and D_3^+, Mon. Not. R. Astron. Soc. 519 (2023) 6333–6348, http://dx.doi.org/10.1093/mnras/stad050.

[33] I.E. Gordon, L.S. Rothman, R.J. Hargreaves, R. Hashemi, E.V. Karlovets, F.M. Skinner, E.K. Conway, C. Hill, R.V. Kochanov, Y. Tan, P. Wcisło, A.A. Finenko, K. Nelson, P.F. Bernath, M. Birk, V. Boudon, A. Campargue, K.V. Chance, A. Coustenis, B.J. Drouin, J.-M. Flaud, R.R. Gamache, J.T. Hodges, D. Jacquemart, E.J. Mlawer, A.V. Nikitin, V.I. Perevalov, M. Rotger, J. Tennyson, G.C. Toon, H. Tran, V.G. Tyuterev, E.M. Adkins, A. Baker, A. Barbe, E. Canè, A.G. Császár, A. Dudaryonok, O. Egorov, A.J. Fleisher, H. Fleurbaey, A. Foltynowicz, T. Furtenbacher, J.J. Harrison, J.-M. Hartmann, V.-M. Horneman, X. Huang, T. Karman, J. Karns, S. Kassi, I. Kleiner, V. Kofman, F. Kwabia-Tchana, N.N. Lavrentieva, T.J. Lee, D.A. Long, A.A. Lukashevskaya, O.M. Lyulin, V.Y. Makhnev, W. Matt, S.T. Massie, M. Melosso, S.N. Mikhailenko, D. Mondelain, H.S.P. Müller, O.V. Naumenko, A. Perrin, O.L. Polyansky, E. Raddaoui, P.L. Raston, Z.D. Reed, M. Rey, C. Richard, R. Tóbiás, I. Sadiek, D.W. Schwenke, E. Starikova, K. Sung, F. Tamassia, S.A. Tashkun, J. Vander Auwera, I.A. Vasilenko, A.A. Vigasin, G.L. Villanueva, B. Vispoel, G. Wagner, A. Yachmenev, S.N. Yurchenko, The HITRAN2020 molecular spectroscopic database, Quant. Spectrosc. Radiat. Transf. 277 (2022) 107949, http://dx.doi.org/10.1016/j.jqsrt.2021.107949.

[34] A.A.A. Azzam, B.M.J. Abou Doud, M.Q.A. Shersheer, B.K.M. Almasri, C.N.M. Bader, A.M.H.A. Baraa O. A. KH. Musleh and, A.W.M. Al Shatarat, B.I.M. Qattan, L.H.M. Hamamsy, A.O.G. Saafneh, M.N.A. ALso'ub, M.M.A. Alkhashashneh, H.O.M. Al-Zawahra, D. Alatoom, M.T.I. Ibrahim, J. Tennyson, S.N. Yurchenko, T. Furtenbacher, A.G. Császár, The 626M24 dataset of validated transitions and empirical rovibrational energy levels of$^{16}O^{12}C^{16}O$, Sci. Data 12 (2025) 532, http://dx.doi.org/10.1038/s41597-025-04755-w.

[35] X. Huang, D.W. Schwenke, R.S. Freedman, T.J. Lee, Ames-2016 line lists for 13 isotopologues of CO_2: Updates, consistency, and remaining issues, J. Quant. Spectrosc. Radiat. Transf. 203 (2017) 224–241.

[36] P.J. Mohr, D.B. Newell, B.N. Taylor, E. Tiesinga, CODATA recommended values of the fundamental physical constants:2022, Rev. Modern Phys. 97 (2025) 025002, http://dx.doi.org/10.1103/RevModPhys.97.025002.

[37] J. Tennyson, The calculation of vibration–rotation energies of triatomic molecules using scattering coordinates, Comput. Phys. Rep. 4 (1986) 1–36.

[38] Z. Bačić, J.C. Light, Theoretical methods for rovibrational states of floppy molecules, Ann. Rev. Phys. Chem. 40 (1989) 469–498, http://dx.doi.org/10.1146/annurev.pc.40.100189.002345.

[39] J.C. Light, T. Carrington Jr., Discrete-Variable Representations and their Utilization, John Wiley & Sons, Ltd, 2000, pp. 263–310.

[40] J.M. Bowman, T. Carrington, H.-D. Meyer, Variational quantum approaches for computing vibrational energies of polyatomic molecules, Mol. Phys. 106 (2008) 2145–2182, http://dx.doi.org/10.1080/00268970802258609.

[41] A.G. Császár, C. Fabri, T. Szidarovszky, E. Mátyus, T. Furtenbacher, G. Czakó, The fourth age of quantum chemistry: molecules in motion, Phys. Chem. Chem. Phys. 14 (2012) 1085–1106, http://dx.doi.org/10.1039/c1cp21830a.

[42] J. Tennyson, Perspective: Accurate ro-vibrational calculations on small molecules, J. Chem. Phys. 145 (2016) 120901, http://dx.doi.org/10.1063/1.4962907.

[43] J. Sarka, B. Poirier, Hitting the trifecta: How to simultaneously push the limits of schrodinger solution with respect to system size, convergence accuracy, and number of computed states, J. Chem. Theory Comput. 17 (2021) 7732–7744, http://dx.doi.org/10.1021/acs.jctc.1c00824.

[44] E.J. Zak, J. Tennyson, O.L. Polyansky, L. Lodi, S.A. Tashkun, V.I. Perevalov, A room temperature CO_2 line list with ab initio computed intensities, J. Quant. Spectrosc. Radiat. Transfer 177 (2016) 31–42, http://dx.doi.org/10.1016/j.jqsrt.2015.12.022.

[45] A.J. Fleisher, H. Yi, A. Srivastava, O.L. Polyansky, N.F. Zobov, J.T. Hodges, Absolute$^{13}C/^{12}C$ isotope amount ratio for vienna PeeDee belemnite from infrared absorption spectroscopy, Nat. Phys. 17 (2021) 889–893, http://dx.doi.org/10.1038/s41567-021-01226-y.

[46] L.S. Rothman, L.D.G. Young, Infrared energy levels and intensities of carbon dioxide-II, J. Quant. Spectrosc. Radiat. Transfer 25 (1981) 505–524, http://dx.doi.org/10.1016/0022-4073(81)90026-.

[47] R.A. Toth, L.R. Brown, C.E. Miller, V.M. Devi, D.C. Benner, Spectroscopic database of CO_2 line parameters: 4300–7000 cm^{-1}, J. Quant. Spectrosc. Radiat. Transfer 109 (2008) 906–921, http://dx.doi.org/10.1016/j.jqsrt.2007.12.004.

[48] J.R. Henderson, J. Tennyson, All the vibrational bound states of H_3^+, Chem. Phys. Lett. 173 (1990) 133–138.

[49] J. Tennyson, B.T. Sutcliffe, The ab initio calculation of the vibrational-rotational spectrum of triatomic systems in the close-coupling approach, with KCN and H_2Ne as examples, J. Chem. Phys. 77 (1982) 4061–4072, http://dx.doi.org/10.1063/1.444316.

[50] B.T. Sutcliffe, J. Tennyson, A general treatment of vibration–rotation coordinates for triatomic molecules, Intern. J. Quantum Chem. 39 (1991) 183–196.

[51] J.R. Henderson, S. Miller, J. Tennyson, Discrete variable representations of large amplitude ro-vibrational states in a generalised coordinate system, J. Chem. Soc. Faraday Trans. 86 (1990) 1963–1968.

[52] J. Tennyson, B.T. Sutcliffe, Variationally exact ro-vibrational levels of the floppy CH_2^+ molecule, J. Mol. Spectrosc. 101 (1983) 71–82.

[53] I.I. Mizus, N.F. Zobov, V.Y. Makhnev, R.I. Ovsyannikov, M.A. Rogov, J. Tennyson, O.L. Polyansky, Approaching experimental accuracy for triatomic spectra using variational calculations: Potential energy and dipole moment surfaces of N_2O, J. Quant. Spectrosc. Radiat. Transfer 344 (2025) 10946, http://dx.doi.org/10.1016/j.jqsrt.2025.109463.

[54] J. Tennyson, Rotational excitation with pointwise vibrational wavefunctions, J. Chem. Phys. 98 (1993) 9658–9668.

[55] J.R. Henderson, J. Tennyson, B.T. Sutcliffe, All the bound vibrational states of H_3^+: a reappraisal, J. Chem. Phys. 98 (1993) 7191–7203.

[56] S.N. Yurchenko, W. Thiel, P. Jensen, Theoretical ROVibrational energies (TROVE): A robust numerical approach to the calculation of rovibrational energies for polyatomic molecules, J. Mol. Spectrosc. 245 (2007) 126–140, http://dx.doi.org/10.1016/j.jms.2007.07.009.

[57] J. Tennyson, B.T. Sutcliffe, Discretisation to avoid singularities in vibration–rotation hamiltonians: a bisector embedding for AB_2 triatomics, Intern. J. Quantum Chem. 42 (1992) 941–952.

[58] S.N. Yurchenko, T.M. Mellor, R.S. Freedman, J. Tennyson, ExoMol molecular line lists XXXIX: Ro-vibrational molecular line list for CO_2, Mon. Not. R. Astron. Soc. 496 (2020) 5282–5291, http://dx.doi.org/10.1093/mnras/staa1874.

[59] S.N. Yurchenko, A. Yachmenev, R.I. Ovsyannikov, Symmetry adapted ro-vibrational basis functions for variational nuclear motion: TROVE approach, J. Chem. Theory Comput. 13 (9) (2017) 4368–4381, http://dx.doi.org/10.1021/acs.jctc.7b00506.

[60] B.V. Noumerov, A method of extrapolation of perturbations, Mon. Not. R. Astron. Soc. 84 (1924) 592–602, http://dx.doi.org/10.1093/mnras/84.8.592.

[61] J.W. Cooley, An improved eigenvalue corrector formula for solving the Schrödinger equation for central fields, Math. Comp. 15 (1961) 363–374, http://dx.doi.org/10.1090/S0025-5718-1961-0129566-X.

[62] J.T. Hougen, P.R. Bunker, J.W.C. Johns, Vibration-rotation problem in triatomic molecules allowing for a large-amplitude bending vibration, J. Mol. Spectrosc. 34 (1970) 136–172, http://dx.doi.org/10.1016/0022-2852(70)90080-9.

[63] J. Tennyson, S.N. Yurchenko, J. Zhang, C.A. Bowesman, R.P. Brady, J. Buldyreva, K.L. Chubb, R.R. Gamache, M.N. Gorman, E.R. Guest, C. Hill, K. Kefala, A.E. Lynas-Gray, T.M. Mellor, L.K. McKemmish, G.B. Mitev, I.I. Mizus, A. Owens, Z. Peng, A.N. Perri, M. Pezzella, O.L. Polyansky, Q. Qu, M. Semenov, O. Smola, A. ov, W. Somogyi, A. Upadhyay, S.O.M. Wright, N.F. Zobov, The release of the ExoMol database: molecular line lists for exoplanet and other hot atmospheres, J. Quant. Spectrosc. Radiat. Transfer 326 (2024) (2024) 109083, http://dx.doi.org/10.1016/j.jqsrt.2024.109083.

[64] M. Pezzella, G. Mitev, S.N. Yurchenko, J. Tennyson, A.O. Mitrushchenkov, A time-independent, variational method for studying the photodissociation of triatomic molecules, Phys. Chem. Chem. Phys. 26 (2024) 27519–27529, http://dx.doi.org/10.1039/D4CP02771J.

[65] G.B. Mitev, S.N. Yurchenko, J. Tennyson, Predissociation dynamics of the hydroxyl radical (OH) based on a five-state spectroscopic model, J. Chem. Phys. 160 (2024) 144110, http://dx.doi.org/10.1063/5.0198241.

[66] M. Pezzella, S.N. Yurchenko, J. Tennyson, A method for calculating temperature-dependent photodissociaiton cross sections and rates, Phys. Chem. Chem. Phys. 23 (2021) 16390–16400, http://dx.doi.org/10.1039/D1CP02162A.

[67] E.V. Karlovets, I.E. Gordon, L.S. Rothman, R. Hashemi, R.J. Hargreaves, G. Toon, A. Campargue, V.I. Perevalov, P. Čermak, M. Birk, G. Wagner, J.T. Hodges, J. Tennyson, S.N. Yurchenko, The update of the line positions and intensities in the line list of carbon dioxide for the HITRAN2020 spectroscopic database, J. Quant. Spectrosc. Radiat. Transfer 276 (2021) 107896, http://dx.doi.org/10.1016/j.jqsrt.2021.107896.

[68] S.A. Tashkun, V.I. Perevalov, R.R. Gamache, J. Lamouroux, CDSD-296, high resolution carbon dioxide spectroscopic databank: An update, J. Quant. Spectrosc. Radiat. Transfer 228 (2019) 124–131, http://dx.doi.org/10.1016/j.jqsrt.2019.03.001.

[69] I.I. Mizus, M.A. Rogov, N.F. Zobov, R.I. Ovsyannikov, E.I. Lebedev, J. Tennyson, O.L. Polyansky, Calculated $^{14}N_2^{16}O$ line intensities using Radau coordinates and an accurate potential energy surface, Mol. Spectrosc. 411- 412 (2025) 112034, http://dx.doi.org/10.1016/j.jms.2025.112034.

[70] X. Huang, R.S. Freedman, S.A. Tashkun, D.W. Schwenke, T.J. Lee, Semi-empirical$^{12}C^{16}O_2$ IR line lists for simulations up to 1500 K and 20 000cm^{-1}, J. Quant. Spectrosc. Radiat. Transfer 130 (2013) 134–146, http://dx.doi.org/10.1016/j.jqsrt.2013.05.018.

[71] L. Lodi, J. Tennyson, Line lists for $H_2{}^{18}O$ and $H_2{}^{17}O$ based on empirically-adjusted line positions and ab initio intensities, J. Quant. Spectrosc. Radiat. Transfer 113 (2012) 850–858, http://dx.doi.org/10.1016/j.jqsrt.2012.02.023.